Appl. Phys. B 85, 301–306 (2006)
DOI: 10.1007/s00340-006-2369-9

Applied Physics B
Lasers and Optics

G. WYSOCKI✉
A.A. KOSTEREV
F.K. TITTEL

Influence of molecular relaxation dynamics on quartz-enhanced photoacoustic detection of CO_2 at $\lambda = 2\,\mu m$

Department of Electrical and Computer Engineering, Rice University, 6100 Main Street, Houston TX 77251, USA

Received: 4 May 2006/Revised version: 19 June 2006
Published online: 14 July 2006 •

ABSTRACT Carbon dioxide (CO_2) trace gas detection based on quartz enhanced photoacoustic spectroscopy (QEPAS) using a distributed feedback diode laser operating at $\lambda = 2\,\mu m$ is performed, with a primary purpose of studying vibrational relaxation processes in the CO_2-N_2-H_2O system. A simple model is developed and used to explain the experimentally observed dependence of amplitude and phase of the photoacoustic signal on pressure and gas humidity. A (1σ) sensitivity of 110 parts-per-million (with a 1 s lock-in time constant) was obtained for CO_2 concentrations measured in humid gas samples.

PACS 07.07.Df; 42.62.Fi; 82.80.Kq; 42.55.Px

1 Introduction

Photoacoustic spectroscopy (PAS) has proved to be a sensitive and reliable technique for detection of trace gases in various applications ([1–3] and references therein). A new approach to the photoacoustic (PA) signal detection was introduced in 2002 by Kosterev et al. [4] In this technique called quartz enhanced photoacoustic spectroscopy (QEPAS) a high Q-factor quartz resonator is used as a resonant sound transducer, which allows sensitive detection of a laser-generated photoacoustic wave. It has been already demonstrated that the application of quartz tuning forks (TFs) as QEPAS based trace gas transducers results in comparable detection sensitivities to traditional PAS offering in addition to all the characteristic features of PAS (e.g. intrinsically zero background and wavelength independence) such advantages as: immunity to ambient acoustic noise emitted from distant sources or measurement of extremely small volume samples ($< 1\,mm^3$) [5]. Application of commercially available TFs resonant at 32 768 Hz makes the overall sensor very cost effective and allows miniaturization of the sensor. Such a relatively high operational modulation frequency introduces an important additional functionality to QEPAS based sensors. In contrast to classical PAS-based sensors, where in order to maximize photoacoustic signal these instruments operate typically at a modulation frequency much smaller than molecular relaxation time of the target species $f \ll 1/\tau_r$ (typically < 1 kHz), the QEPAS based sensor detecting the PA signal at ~ 32 kHz preserves the capability to distinguish between different molecular relaxation times. This can be used as an additional spectroscopic parameter for discrimination between PA signals originating from molecular species with overlapping absorption spectra [6]. The same technique can be also applied for measurement of molecular relaxation times associated with different vibration–translation (V–T) and vibration–vibration (V–V) energy transfer mechanisms characteristic for a particular molecular gas mixture under investigation.

The development of laser spectroscopy strongly relies on the availability of suitable laser sources, which allow the design of sensitive, robust and compact trace gas sensor instrumentation. The excellent choice of high spectral quality, reliable and cost-effective telecommunication diode lasers in the near infrared (near-IR) spectral region, make them very attractive sources for spectroscopic applications. However the strength of overtone and combination band molecular transitions in near-IR is several orders of magnitude smaller than the fundamental transitions in the mid-infrared (mid-IR) region. The commercial availability of reliable semiconductor laser sources, such as quantum cascade lasers, in the mid-IR is still limited. This strongly limits their range of applications, despite their superior suitability for trace gas concentration measurements. Continuous wave distributed feedback diode lasers emitting at $\sim \lambda = 2\,\mu m$, which have recently become a commercial product are an interesting alternative to telecommunications diode lasers in spectroscopic applications. We have chosen a diode laser emitting at $\sim 2\,\mu m$ for QEPAS detection of carbon dioxide CO_2, which at this wavelength has 10 times stronger molecular transitions than the strongest absorption lines available in the telecommunication E-band at $\sim 1.43\,\mu m$ (see Fig. 1).

2 Experimental

2.1 *Wavelength selection*

The strongest CO_2 molecular absorption lines around $\lambda = 2\,\mu m$ are in the R-branch of the $2\nu_1 + \nu_3$ band (see Fig. 1). The diode laser selected for this experiment (NTT Electronics, model: KELD1G5B2TA) can be tuned between $4982\,cm^{-1}$ and $4993\,cm^{-1}$ by changing the temperature of the laser submount between 41 °C and 12 °C respectively. Fine laser frequency tuning can be performed by chang-

✉ Fax: +1-713-348-5686, E-mail: gerardw@rice.edu

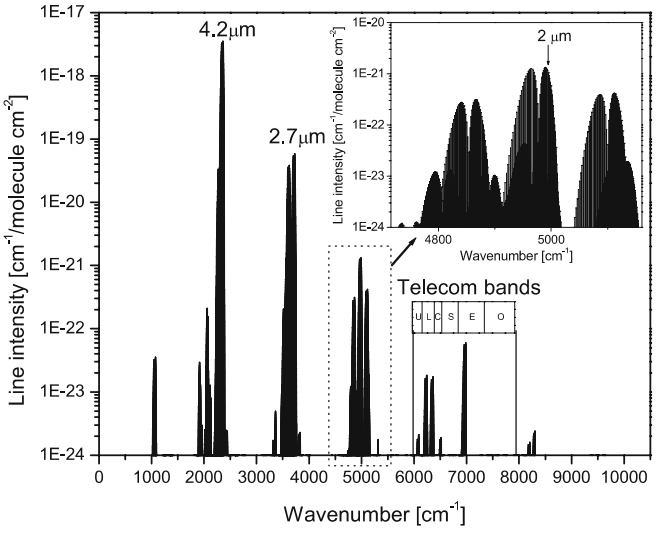

FIGURE 1 Molecular absorption line intensity spectrum of CO_2 calculated using the HITRAN 2000 database

ing the laser current with a wavelength tuning coefficient of $\mathrm{d}\lambda/\mathrm{d}I \cong 18.08\,\mathrm{nm/A}$. Figure 2 depicts a HITRAN 2000 simulation of CO_2 absorption features within the tuning range of the laser radiation, together with possible interference from H_2O. The calculation is done for average atmosphere CO_2 concentrations of 350 ppm and 100% humidity for an absorption pathlength of 1 m, and a pressure of 300 Torr which was found to be optimum for CO_2 QEPAS-based monitoring in dry air. As shown in Fig. 2 the strongest lines $R16$ and $R18$, with line strengths of $S = 1.33 \times 10^{-21}\,\mathrm{cm^{-1}/molecule\,cm^{-2}}$ and $S = 1.30 \times 10^{-21}\,\mathrm{cm^{-1}/molecule\,cm^{-2}}$ respectively, are free of H_2O interference and can be used for sensitive CO_2 concentration measurements. Within the overall laser tuning range one can also target several ammonia (NH_3) absorption lines with a line strength of the order of $S = 7.7 \times 10^{-21}\,\mathrm{cm^{-1}/molecule\,cm^{-2}}$ (~ 6 times stronger than the available CO_2 lines), which can be used for simultaneous multi-species measurement with a single diode laser source.

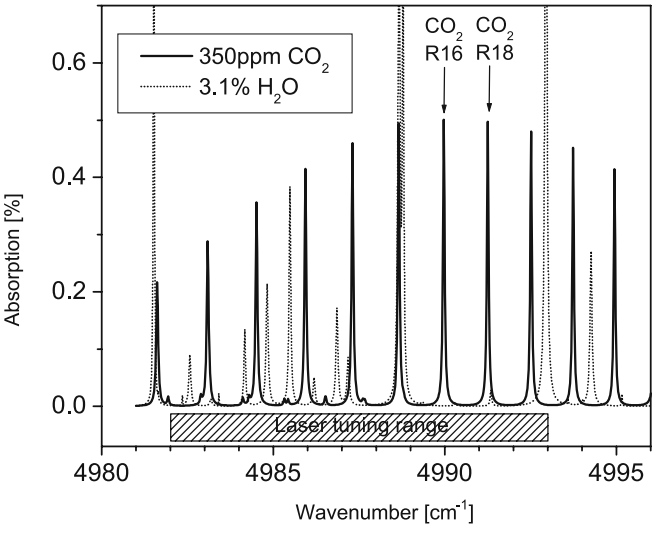

FIGURE 2 CO_2 ($2\nu_1 + \nu_3$ band) and H_2O absorption spectrum calculated within the spectral tuning range of the 2 μm diode laser

However, this is not an objective of the current work and will be published elsewhere.

2.2 *Sensor architecture*

The sensor platform is schematically shown in Fig. 3. The diode laser, enclosed in a can-type package, was placed in a non-hermetic thermoelectrically cooled laser head (Thorlabs, model: TCLDM9). To avoid condensation of atmospheric water on the laser chip the temperature was always kept above the dew point. Coarse wavelength tuning was performed by variation of the laser heat sink temperature. Fine laser frequency tuning and fast wavelength modulation was performed using laser current modulation. An appropriate modulation waveform was supplied from an external computer controlled function generator. The laser beam was collimated using an 8 mm diameter aspherical lens with an effective focal length of 8 mm (material: corning glass C0550). The collimated laser beam was refocused through an Al_2O_3 window between the prongs of the TF enclosed in a compact gas cell ($\sim 1\,\mathrm{cm^3}$) using a Ø25 mm BK7 lens with a 75 mm focal length. Upon exiting the gas chamber through the second Al_2O_3 window the laser beam was directed onto a power meter used for PA signal normalization. The laser was supplied with an ~ 80 mA current at which it could deliver ~ 5.5 mW of optical power. Using the optical power measurement before and after the gas cell the effective laser power between the TF prongs is estimated to be at the level of ~ 4.6 mW. For spectral measurements a wavelength modulation technique with 2nd harmonic detection was applied. The frequency of the laser radiation was modulated with a sinusoidal signal at frequency $f_0/2$, where f_0 is the TF resonance frequency. The modulation depth was optimized with respect to the working pressure in order to match the width of the pressure broadened target absorption line. A TF with a resonance frequency of 32.768 kHz (in vacuum) is used as a QEPAS transducer. For precise PA signal phase measurements the micro resonator commonly used in QEPAS applications [7] was not used in this work in order to avoid an introduction of an additional PA phase shift. The TF piezoelectric current was amplified in a transimpedance amplifier with a gain of 10^7 V/A and measured by a lock-in amplifier (Signal Recovery, model: 7265).

For an investigation of the influence of the H_2O content in a sample gas mixture on the CO_2 PA signal, a gas moisturizer with a diluter was used at the sampling inlet. Part of the calibrated gas mixture flow passed through the temperature stabilized H_2O bath to achieve a saturated H_2O vapor pressure. The temperature of the bath was stabilized and kept below room temperature ($\sim 16.4\,^\circ$C) to avoid condensation on the walls of the entire system. Dry and moist flows of the calibrated gas mixture were delivered to the diluter inlets, which allowed the concentration of the H_2O vapor in the sample gas to be varied with a maximum dilution ratio of 10. To avoid errors in estimation of the H_2O concentration on the basis of the dilution ratio, an additional 15 cm absorption cell was installed inline with the QEPAS cell and the H_2O concentration was monitored using direct absorption measurements with a telecom diode laser targeting H_2O absorption line at $7306.736\,\mathrm{cm^{-1}}$. A PC computer equipped with a data acquisition card (National Instruments, model: DAQ6062E) was

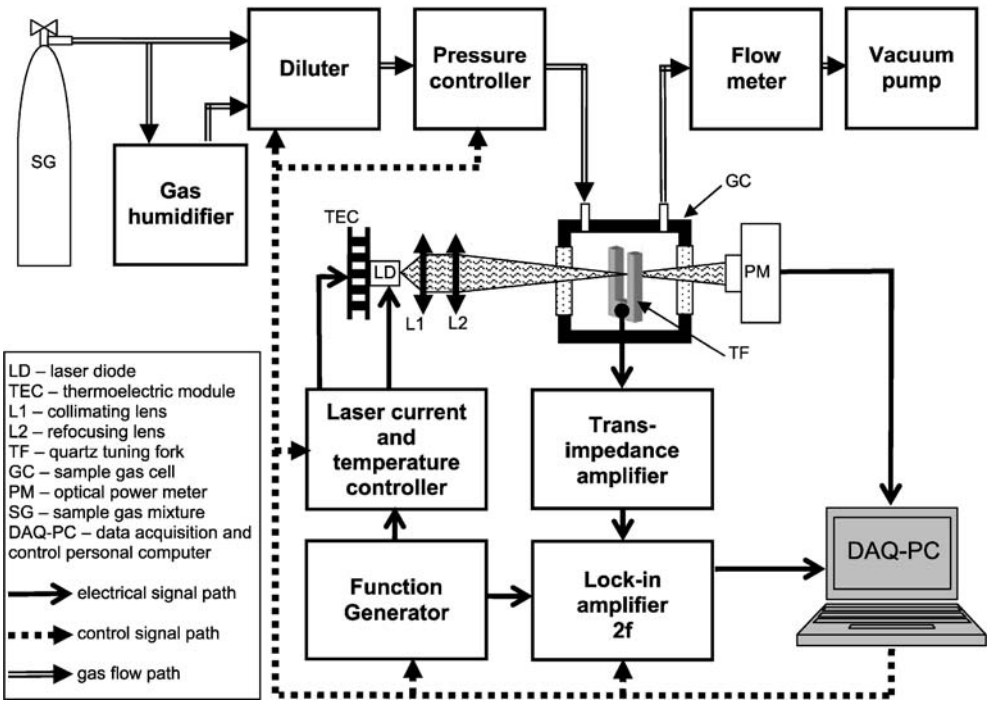

FIGURE 3 Schematic configuration of the QEPAS based CO_2 sensor

used to control the instrumentation and log the measurement data.

2.3 *Optimization of the sensor performance*

Sensor optimization is performed by appropriate selection of the working pressure and wavelength modulation depth of the diode laser source. Calibration curves were collected for two different gas mixtures:

1. 1% CO_2 in dry N_2
2. human breath sample (approximately 4% CO_2 in air with close to 100% relative humidity).

At each pressure level the resonance frequency and Q-factor of the TF were measured and the QEPAS modulation frequency adjusted accordingly. The results are presented in Fig. 4. For convenient comparison the curves are normalized to the total maximum value and the values of the x-axes are presented in the same range. The difference between the optimum working conditions for both situations visible in Fig. 4a and b is related to the V–T relaxation mechanisms which are different in the two mixtures. Due to much slower vibrational relaxation in a dry mixture the heat release can not efficiently follow the fast modulation of the incident laser radiation. In this case the only way to increase the relaxation rate is by increasing the working pressure. In QEPAS however the TF Q-factor decreases with increasing pressure, which causes the detected PA signal to decrease. Interaction of these two mechanisms results in the characteristic maxima for the calibration curves shown in Fig. 4a. Behavior of the PA signal becomes different for a moist CO_2 mixture. The optimum working pressure shifts from 300 Torr in dry gas to 60 Torr in humid gas. This shift indicates that the relaxation process becomes fast and does not limit the generation of the PA signal. In this pressure range the PA signal is mainly determined by the absorption coefficient, which decreases at reduced pressures (below $\sim$ 100 Torr). Therefore the characteristic maximum of the calibration curves shown in Fig. 4b arises mainly from an interaction of the latter mechanism with the Q-factor increasing at reduced pressures. The strong enhancement of the relaxation process in the presence of H_2O vapor causes a substantial improvement of the sensor minimum detection limit. The optimum pressure for the humid CO_2 mixture was chosen to be the best working condition for sensitive investigation of the influence of the H_2O vapor on the overall vibrational relaxation process in such a gas system. At this pressure the TF's Q-factor was $\sim$ 21 000 and its resonance frequency was $f_0 = 32\,762.57$ Hz

2.4 *Influence of* H_2O *on* CO_2 *relaxation processes*

All energy transfer paths in a CO_2-N_2-H_2O gas mixture contributing to the relaxation process from the excited CO_2 $2\nu_1 + \nu_3$ state are complex, and therefore a complete identification of such processes will not be possible. However in order to investigate the influence of H_2O content on the overall relaxation time one can develop a simplified model of energy transfer in such a gas mixture (see Fig. 5). We can assume that the relaxation process in a CO_2-N_2 gas mixture can be characterized by the relaxation time $\tau_1 = 1/k_1$ (where k_1 is a relaxation rate constant). This process is relatively slow, which results in a weak PA signal for a dry CO_2 mixture at reduced pressures < 100 Torr (as shown in Fig. 4a). This might be related to slow vibrational relaxation of CO_2 and also to a partial energy transfer to N_2 and subsequent trapping of the energy in a metastable vibrational excited state of N_2, which can occur in a CO_2-N_2 system [9–12].The presence of H_2O opens an additional relaxation path. V–T relaxation in H_2O is known to be very fast and can be represented by a relaxation time $\tau_3 = 1/k_3$. This is connected with its ability to create an efficient V–T and V–V collisional energy exchange

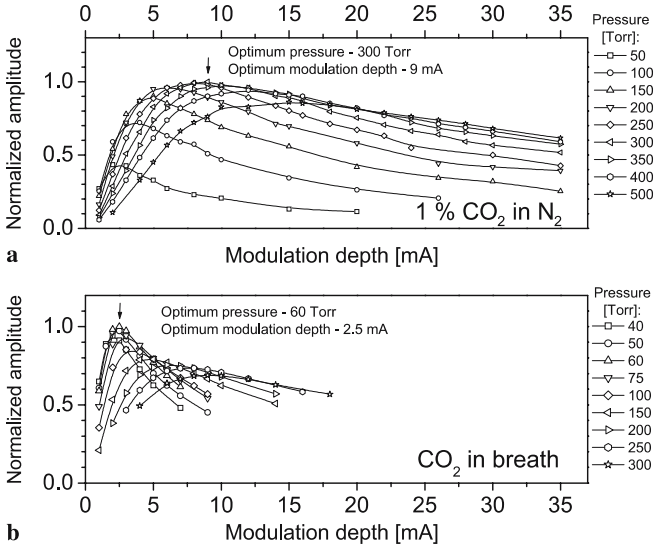

FIGURE 4 Sensor optimization curves acquired at different operation pressures for (**a**) a dry reference gas mixture of 1% CO_2 in N_2 and (**b**) a humid sample ($\sim$ 3%–4% of CO_2 in human breath)

with other molecules, and makes the H_2O a very good molecular energy deactivation catalyst[10, 13]. In our simplified model we assume a near-resonant energy transfer from the CO_2-N_2 system to H_2O with a rate constant k_2, which is proportional to the H_2O concentration ($k_2 \sim [H_2O]$).

The PA signal is formed due to a change in gas pressure given by $\frac{dP}{dt} = \frac{C}{nR}\frac{dH}{dt}$[14], which is proportional to the rate of heat $\frac{dH}{dt}$ produced per unit volume during relaxation of the molecular vibrational energy. The constants C, n and R are the total heat capacity of the gas at constant volume, the number of moles of the gas and the gas constant respectively. In our system the rate of the produced heat can be denoted as $\frac{dH}{dt} = E\left(k_1 N^* + k_3 N_1^*\right)$, where N^* and N_1^* are the number of excited molecules in the CO_2-N_2 system and in H_2O respectively, and E is the energy to be deactivated. In order to determine the dependence of the PA signal on the water concentration [H_2O] it is necessary to solve the following equation:

$$\frac{dP}{dt} = \frac{C}{nr} R\left(k_1 N^* + k_3 N_1^*\right) . \tag{1}$$

To calculate N^* and N_1^* the following rate equations must be solved:

$$\frac{dN^*}{dt} = W - k_1 N^* - k_2 N^* . \tag{2}$$

$$\frac{dN_1^*}{dt} = k_2 N^* - k_3 N_1^* \tag{3}$$

where W is the rate of molecular excitation by the laser. For a sinusoidal modulation of the laser intensity $W = W_0\left(a + be^{i\omega t}\right)$with a frequency $\omega = 2\pi f$ we obtain the following solutions:

$$N^*(t) = W_0\tau_{12}\left(a + \frac{b}{\sqrt{1+(\omega\tau_{12})^2}} e^{i(\omega t - \varphi_{12})}\right) \tag{4}$$

$$N_1^*(t) = W_0\tau_{12}\tau_3 k_2 \times\left(a + \frac{b}{\sqrt{1+(\omega\tau_{12})^2}\sqrt{1+(\omega\tau_3)^2}} e^{i(\omega t - \varphi_{12} - \varphi_3)}\right) \tag{5}$$

where $\tau_{12} = \frac{1}{k_1 + k_2}$, $\varphi_{12} = \arctan(\omega\tau_{12})$, and $\varphi_3 = \arctan(\omega\tau_3)$. Only the oscillatory part of laser induced pressure change contributes to the measured PA signal. Using (1), (2) and (3) we can calculate a general expression for the oscillating PA signal:

$$P(t) = \frac{P_0\tau_{12}}{\sqrt{1+(\omega\tau_{12})^2}}\left(k_1 + \frac{k_2}{\sqrt{1+(\omega\tau_3)^2}} e^{-i\varphi_3}\right) e^{i\left(\omega t - \frac{\pi}{2} - \varphi_{12}\right)} \tag{6}$$

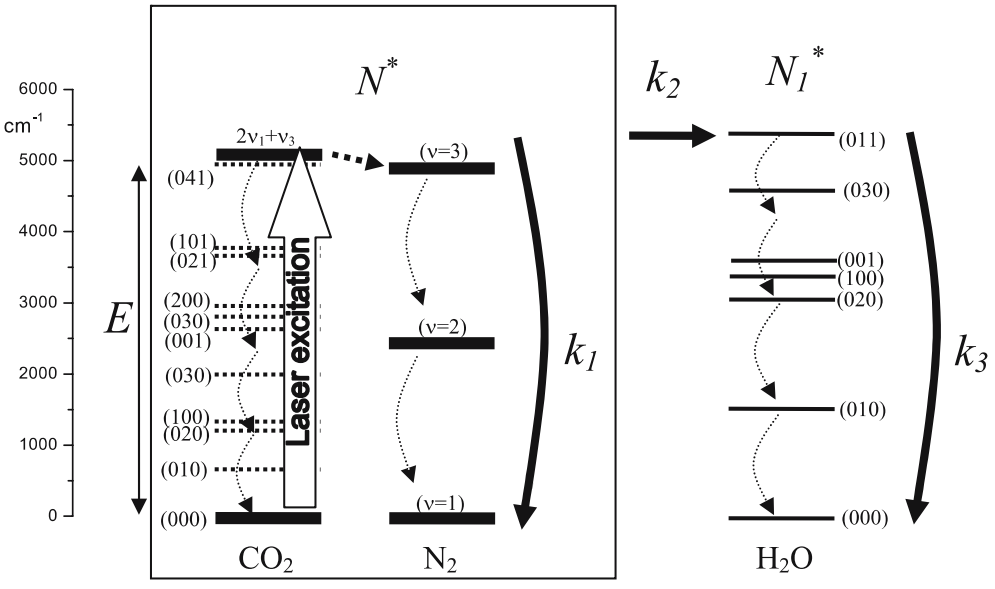

FIGURE 5 Simplified model of molecular vibration energy transfer in CO_2 -N_2-H_2O gas mixture (energy levels from [8])

where $P_0 = \frac{CW_0bE}{nR}$. This expression can be further simplified if the relaxation in H_2O can be considered instantaneous, which is a good approximation when $k_3 \gg k_2 > k_1$. In this case for $\omega\tau_3 \ll 1$ the (6) can be reduced to:

$$P(t) = \frac{P_0}{\sqrt{1+(\omega\tau_{12})^2}} e^{i\left(\omega t - \frac{\pi}{2} - \varphi_{12}\right)}. \quad (7)$$

The measurement data of the amplitude and phase of the PA signal as a function of H_2O concentration, acquired with a QEPAS system are shown in Fig. 6a and b. To perform an accurate phase measurements of the PA signal an instrumental phase shift φ_0 introduced by the measurement system must be determined. As mentioned previously the measurements were performed using WM technique and 2nd harmonic detection. Therefore φ_0 of the 2nd harmonic of the optical input signal was determined by performing direct absorption measurement using a high concentration CO_2 mixture at the same pressure as for QEPAS measurements. Such a measurement yielded $\varphi_0 = 198°$.

Assuming that $C_1 = \frac{k_1}{\omega}$ and φ_3 are constant values and $C_2 x = \frac{k_2(x)}{\omega}$ is a function of H_2O concentration x, (6) yielded the following expression for a PA signal amplitude as a function of x:

$$|P|(x) = P_0 \times \frac{\sqrt{C_1^2 + 2C_1C_2\frac{1}{\sqrt{1+\tan^2(\varphi_3)}}\cos(\varphi_3)x + \frac{1}{1+\tan^2(\varphi_3)}C_2^2x^2}}{\sqrt{1+(C_1+C_2x)^2}} \quad (8)$$

and for the PA signal phase as a function of x:

$$\varphi(x) = \varphi_0 - \frac{\pi}{2} - \arctan\left(\frac{1}{C_1+C_2x}\right) - \arctan\left(\frac{C_2\sin(\varphi_3)x}{C_1\sqrt{1+\tan^2(\varphi_3)}+C_2\cos(\varphi_3)x}\right). \quad (9)$$

Parameters obtained from the best fit satisfying both equations ($P_0 = 283$, $C_1 = 0.035$, $C_2 = 145$, $\varphi_3 = 0.25\text{rad} = 14.3°$) allow us to calculate the following values of characteristic relaxation time constants at 60 Torr: $\tau_1 = 139\,\mu s$ and $\tau_3 = 1.24\,\mu s$ (this yields $\tau_1 \approx 11\,\mu s\,atm$ and $\tau_3 \approx 0.1\,\mu s\,atm$). The net relaxation time can be varied between these values by changing the humidity of the sample gas mixture. Even though a complete analysis of the relaxation process for the combination band and overtone vibration energy levels in such a gas system would be complex, the simplified relaxation model allowed us to obtain an excellent fit of the measured amplitude and phase functions (with correlation coefficients of 0.9956 and 0.9987 respectively) resulting in realistic values of relaxation times τ_1 and τ_3. This also confirms that the approximation assumed to derive (7) is valid and can be used for an approximation of the measurement results.

An additional feature of the phase characteristic described by (9), which does not depend on the CO_2 concentration, is its capability of indirect monitoring of the H_2O concentration. This can be done for a relatively limited range of concentrations, because as it is depicted in Fig. 6b the curve has a saturating characteristic. However, for atmospheric chemistry study, in which CO_2 plays an important rule as a greenhouse gas and a major component of the carbon cycle, monitoring of typical atmospheric humidity levels can be useful.

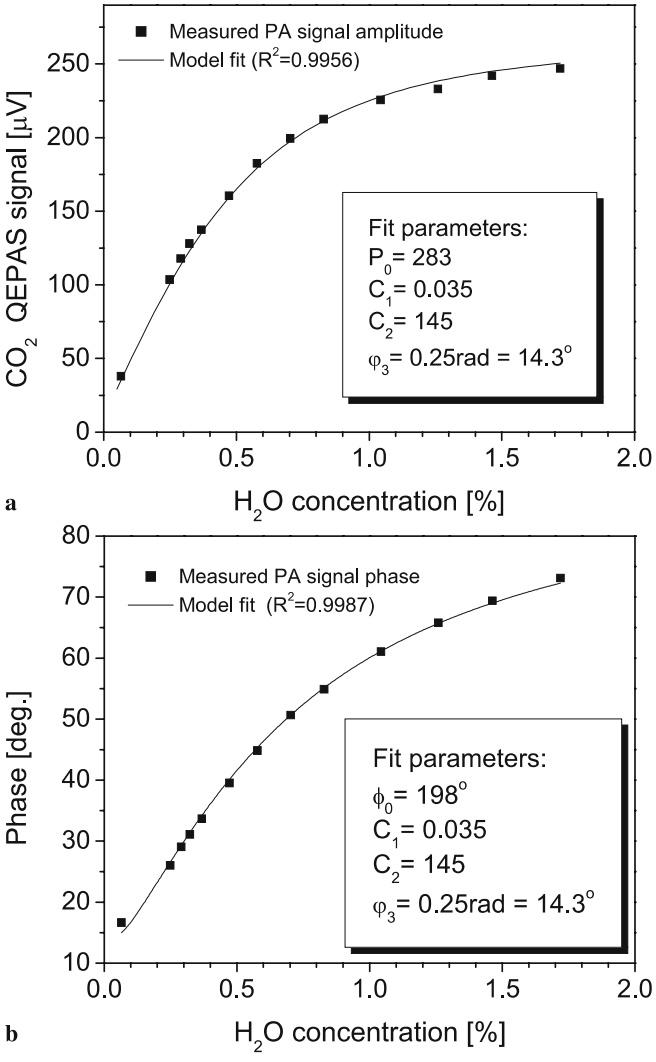

FIGURE 6 Amplitude (**a**) and phase (**b**) of the CO_2 PA signal as a function of H_2O concentration. Data measured by the QEPAS sensor (*squares*) are fitted with the calculated model curves (*solid lines*)

2.5 CO_2 *detection limit*

The minimum detection limit of the sensor was evaluated at an optimum pressure of 60 Torr by recording a spectrum of 1% CO_2 in the air calibration mixture humidified by adding 1.72% of H_2O ($\sim$ 55% relative humidity). A WM $2f$ signal was recorded by performing a 180 points scan of a dc component of the laser current from 79 mA to 83.5 mA. The phase reference of the lock-in amplifier was adjusted to be in-phase with the PA signal and measurements were acquired using a 1s time constant. The resulting spectrum of the $R18$ CO_2 line is presented in Fig. 7. The noise level could be directly calculated as a standard deviation of the measurements acquired by lock-in as an out-of-phase signal. A single point standard deviation returns a value of $1\sigma = 2.7\,\mu V$ ($\sim 4.8\,\mu V/\sqrt{Hz}$) and yields for 1% CO_2 con-

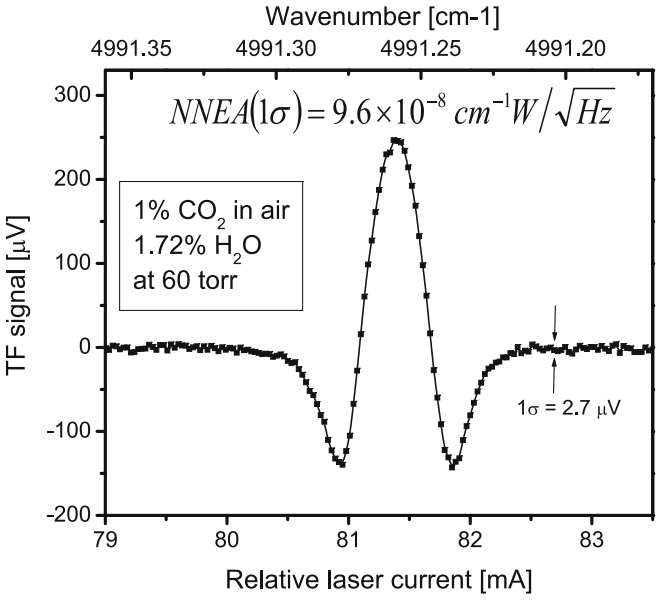

FIGURE 7 The second harmonic PA signal spectrum of the CO_2 *R*18 line acquired with a 2 μm laser diode based QEPAS sensor

centration a signal to noise ratio of 91.5. This translates into a minimum detection limit of ∼ 110 ppm of CO_2. A normalized noise equivalent absorption coefficient (NNEA) of the PA signal normalized to available laser power, absorption coefficient and measurement bandwidth yields a $\mathrm{NNEA}(1\sigma) = 9.6 \times 10^{-8}\,\mathrm{cm^{-1}W}/\sqrt{\mathrm{Hz}}$. The noise level in the QEPAS spectrum is known to be primarily determined by the fundamental thermal noise of the TF [5]. The theoretical thermal noise of the TF can be estimated as a thermal noise of TF resistance measured at the resonance frequency. For a measured TF resistance value of 47.3 kΩ at 60 Torr the calculation of the theoretical noise level at the output of the transimpedance amplifier results in a value of $\sim 4.2\,\mu\mathrm{V}/\sqrt{\mathrm{Hz}}$ (the noise level measured by the lock-in amplifier in one of the quadrature components). This value is in a good agreement with the noise level determined from the spectral measurements, which confirms the fact that the reported QEPAS sensor sensitivity is mainly limited by the TF thermal noise floor.

3 Summary

A QEPAS CO_2 trace gas sensor employing a diode laser operating at $\lambda = 2\,\mu\mathrm{m}$ as the spectroscopic source has been developed. The sensitivity to the CO_2 concentration was determined for a gas mixture containing 1.72% H_2O, which is used to enhance the CO_2 molecular relaxation process. The detection limit of 110 ppm of CO_2 (for 1 s lock-in time constant), which corresponds to a normalized value of $\mathrm{NNEA}(1\sigma) = 9.6 \times 10^{-8}\,\mathrm{cm^{-1}W}/\sqrt{\mathrm{Hz}}$ was achieved. Even without further sensitivity enhancement of the sensor performance, the reported system is applicable for detection of CO_2 elevated above the average atmospheric level of 350 ppm with simultaneous humidity monitoring (e.g. in medical or biological studies of the respiration processes, fermentation and cellular respiration). Applications such as monitoring of fossil fuels combustion or volcanic outgassing, where strongly elevated CO_2 must be measured with high accuracy, can also take advantage of the large QEPAS dynamic range, compactness and high potential for further miniaturization of the gas sensor.

The system was also designed to investigate the ability of the QEPAS to perform photoacoustic measurements of molecular relaxation times. Using QEPAS signal measurements obtained for different concentrations of a H_2O in CO_2 sample gas mixture, and applying a simplified theoretical model of the molecular energy transfer for the CO_2-N_2-H_2O gas system, a calculation of the characteristic relaxation times was demonstrated.

The detection limit of the sensor can be further improved by a factor of ∼ 8–10 by adding an acoustic microresonator to the TF assembly [5, 7], and an additional factor of ∼ 2 or more by "recycling" of the laser power within the system by redirecting the beam back to the TF sensor. These modifications were not applied in the current version of the sensor to avoid introduction of additional phase shift effects. With the implementation of further incremental sensor modifications their influence on the QEPAS signal amplitude and phase lag will be further investigated.

ACKNOWLEDGEMENTS Financial support for the work performed by the Rice group was provided by the National Aeronautics and Space Administration (NASA), DARPA via a subaward from Pacific Northwest National Laboratory (PNNL), Richfield, WA, the Texas Advanced Technology Program, the Robert Welch Foundation, and the Office of Naval Research via a subaward from Texas A&M University.

REFERENCES

1 M.W. Sigrist, Rev. Sci. Instrum. **74**, 486 (2003)
2 A. Miklós, P. Hess, Z. Bozóki, Rev. Sci. Instrum. **72**, 1937 (2001)
3 M.W. Sigrist, C. Fischer, J. Phys. IV France **125**, 619 (2005)
4 A.A. Kosterev, Y.A. Bakhirkin, R.F. Curl, F.K. Tittel, Opt. Lett. **27**, 1902 (2002)
5 A.A. Kosterev, F.K. Tittel, D. Serebryakov, A. Malinovsky, I. Morozov, Rev. Sci. Instrum. **76**, 043 105 (2005)
6 A.A. Kosterev, Y.A. Bakhirkin, F.K. Tittel, S. Blaser, Y. Bonetti, L. Hvozdara, Appl. Phys. B **78**, 673 (2004)
7 D. Weidmann, A.A. Kosterev, F.K. Tittel, N. Ryan, D. McDonald, Opt. Lett. **29**, 1837 (2004)
8 G. Herzberg, *Infrared and Raman Spectra of Polyatomic Molecules* (D. van Nostrand, New York, 1945)
9 M. Hammerich, A. Ólafsson, J. Henningsen, Chem. Phys. **163**, 173 (1992)
10 R.L. Taylor, S. Bitterman, Rev. Mod. Phys. **41**, 26 (1969)
11 A.D. Wood, M. Camac, E.T. Gerry, Appl. Opt. **10**, 1877 (1971)
12 M.A. Moeckli, C. Hilbes, M.W. Sigrist, Appl. Phys. B **67**, 449 (1998)
13 A. Veres, Z. Bozóki, Á. Mohácsi, M. Szakáll, G. Szabó, Appl. Spectrosc. **57**, 900 (2003)
14 T.F. Hunter, D. Rumbles, M.G. Stock, J. Chem. Soc. Faraday Trans. 2 **70**, 1010 (1974)